

Supporting Information

Co-crystal AX·(H₃C₃N₃O₃) (A = Na, Rb, Cs; X = Br, I): a series of strongly anisotropic alkali halide cyanurates with planar structural motif and large birefringence

Jinhui Wang,^a Xinyuan Zhang,^{*a} Fei Liang,^{*b} Zhanggui Hu^a and Yicheng Wu^{a, b}

^a Tianjin Key Laboratory of Functional Crystal Materials, Institute of Functional Crystals, Tianjin

University of Technology, Tianjin 300384, China.

^b State Key Laboratory of Crystal Materials and Institute of Crystal Materials, Shandong University,

Jinan 250100, China.

Contents.

Table S1. Fractional atomic coordinates ($\times 10^4$) and equivalent isotropic displacement parameters ($\text{\AA}^2 \times 10^3$) of **I**.

Table S2. Fractional atomic coordinates ($\times 10^4$) and equivalent isotropic displacement parameters ($\text{\AA}^2 \times 10^3$) of **II**.

Table S3. Fractional atomic coordinates ($\times 10^4$) and equivalent isotropic displacement parameters ($\text{\AA}^2 \times 10^3$) of **III**.

Table S4. Anisotropic displacement parameters ($\text{\AA}^2 \times 10^3$) of **I**.

Table S5. Anisotropic displacement parameters ($\text{\AA}^2 \times 10^3$) of **II**.

Table S6. Anisotropic displacement parameters ($\text{\AA}^2 \times 10^3$) of **III**.

Table S7. Selected bond lengths [\AA] of **I - III**.

Table S8. Selected bond angles ($^\circ$) of **I - III**.

Table S9. The infrared vibrations and assignments of **I - IV** in detail (Vibrational frequencies/ cm^{-1}).

Figure S1. The calculated and experimental PXRD patterns for (a) **I**, (b) **II**, (c) **III** and (d) **IV**.

Figure S2. EDS analysis of (a) **I**, (b) **II**, (c) **III** and (d) **IV**.

Figure S3. The TG and DSC curves of (a) **I**, (b) **II**, (c) **III** and (d) **IV**.

Figure S4. The IR spectra of (a) **I**, (b) **II**, (c) **III** and (d) **IV**.

Figure S5. The Raman spectra of (a) **I**, (b) **II**, (c) **III** and (d) **IV**.

Figure S6. Photographs of crystal (a) **I**, (b) **II**, (c) **III** and (d) **IV** for the measurement of birefringence.

Figure S7. Calculated band structures (a) and the partial density of states of constituent atoms in **IV** (b).

Figure S8. The conjugated π -bond state around -5 eV and anti- π bond state around 4 eV on $\text{H}_3\text{C}_3\text{N}_3\text{O}_3$ neutral molecule.

Figure S9. Calculated band structures of (a) **I**, (b) **II** and (c) **III**.

Figure S10. The partial density of states of constituent atoms in (a) **I**, (b) **II** and (c) **III**.

Figure S11. The comparison between $\text{Na}_3(\text{C}_3\text{N}_3\text{O}_3)$ and $\text{Ba}_2\text{M}(\text{C}_3\text{N}_3\text{O}_3)_2$ series ($\text{M} = \text{Mg}, \text{Ca}, \text{Sr}, \text{Ba}$).

Figure S12. The p - π -interaction between Br 4*p* orbitals and π -bond on cyanuric molecules.

Figure S13. The simulated refractive indexes of (a) **I**, (b) **II** and (c) **III**.

1. Supplementary Tables.

Table S1. Fractional atomic coordinates ($\times 10^4$) and equivalent isotropic displacement parameters

($\text{\AA}^2 \times 10^3$) of **I**.

Atom	<i>x</i>	<i>y</i>	<i>z</i>	$U_{(\text{eq})}^{\text{a}}$
Br1	13781.1(11)	4365.5(7)	2500	29.3(2)
Rb1	8652.7(10)	2874.6(7)	2500	31.2(2)
O1	8871(5)	5596(4)	3789(3)	35.1(10)
O2	3075(7)	7500	5000	41.2(16)
N1	8882(8)	7500	5000	22.9(14)
N2	5955(6)	6482(5)	4424(4)	26.5(12)
C1	7961(7)	6460(6)	4360(4)	23.4(13)
C2	4893(10)	7500	5000	24.8(18)

^a $U_{(\text{eq})}$ is defined as one-third of the trace of the orthogonalized U_{ij}

tensor.

Table S2. Fractional atomic coordinates ($\times 10^4$) and equivalent isotropic displacement parameters ($\text{\AA}^2 \times 10^3$) of **II**.

Atom	<i>x</i>	<i>y</i>	<i>z</i>	$U_{(\text{eq})}^{\text{a}}$
I1	3499.4(5)	2500	10663.9(2)	14.56(12)
Rb1	4526.5(7)	2500	7967.5(4)	14.88(15)
O2	3438(4)	5255(4)	3225(2)	18.0(7)
O1	2901(5)	2500	6067(3)	16.9(10)
N1	3310(5)	3893(5)	4657(3)	12.9(7)
N2	3535(7)	2500	3219(3)	15.3(11)
C1	3160(7)	2500	5189(4)	14.4(13)
C2	3422(5)	3980(6)	3659(3)	13.7(9)

^a $U_{(\text{eq})}$ is defined as one-third of the trace of the orthogonalized U_{ij} tensor.

Table S3. Fractional atomic coordinates ($\times 10^4$) and equivalent isotropic displacement parameters ($\text{\AA}^2 \times 10^3$) of **III**.

Atom	<i>x</i>	<i>y</i>	<i>z</i>	$U_{\text{(eq)}}^{\text{a}}$
Cs1	11319.2(8)	2106.4(6)	7500	30.7(2)
Br1	6240.8(13)	611.4(10)	7500	32.6(3)
O1	8703(6)	4378(6)	6152(4)	42.4(12)
O2	2939(10)	2500	5000	44.8(18)
N1	8730(11)	2500	5000	28.6(16)
N2	5818(8)	3490(6)	5563(4)	29.4(12)
C1	7794(10)	3525(8)	5622(5)	29.5(14)
C2	4735(14)	2500	5000	28.6(19)

^a $U_{\text{(eq)}}$ is defined as one-third of the trace of the orthogonalized U_{ij} tensor.

Table S4. Anisotropic displacement parameters ($\text{\AA}^2 \times 10^3$) of **I**.

Atom	U_{11}	U_{12}	U_{33}	U_{23}	U_{13}	U_{12}
Br1	27.3(4)	26.9(4)	33.6(6)	0	0	-1.5(3)
Rb1	31.4(4)	24.4(4)	38.0(6)	0	0	2.6(4)
O1	28.2(19)	41(2)	36(3)	-15.1(19)	4.3(19)	4.0(19)
O2	12(2)	46(4)	65(5)	-7(3)	0	0
N1	9(3)	30(3)	30(4)	-7(3)	0	0
N2	16(2)	27(2)	37(4)	-8(2)	-1(2)	-4(2)
C1	22(3)	30(3)	19(3)	3(3)	1(2)	-1(2)
C2	21(4)	28(4)	26(5)	-1(4)	0	0

^a $U_{(\text{eq})}$ is defined as one-third of the trace of the orthogonalized U_{ij} tensor.

Table S5. Anisotropic displacement parameters ($\text{\AA}^2 \times 10^3$) of **II**.

Atom	U_{11}	U_{12}	U_{33}	U_{23}	U_{13}	U_{12}
I1	16.4(2)	16.8(2)	10.52(17)	0	0.24(14)	0
Rb1	13.0(3)	20.9(4)	10.7(2)	0	0.7(2)	0
O2	24.4(16)	11.6(17)	18.1(14)	4.2(13)	3.1(12)	-0.3(14)
O1	18(2)	23(3)	10.3(19)	0	-0.8(16)	0
N1	14.4(17)	9(2)	14.9(16)	-2.3(15)	-0.1(13)	1.9(15)
N2	22(3)	16(3)	8(2)	0	2(2)	0
C1	9(3)	20(4)	14(3)	0	-1(2)	0
C2	11.4(19)	17(3)	12.4(18)	0.2(17)	-2.7(15)	-1.5(19)

^a $U_{(\text{eq})}$ is defined as one-third of the trace of the orthogonalized U_{ij} tensor.

Table S6. Anisotropic displacement parameters ($\text{\AA}^2 \times 10^3$) of **III**.

Atom	U_{11}	U_{12}	U_{33}	U_{23}	U_{13}	U_{12}
Cs1	31.3(4)	26.7(3)	34.2(3)	0	0	1.9(2)
Br1	28.8(5)	30.7(5)	38.3(5)	0	0	-0.7(4)
O1	34(3)	42(3)	50(3)	-14(2)	-6(2)	-8(2)
O2	19(4)	59(5)	56(4)	-5(4)	0	0
N1	23(4)	31(4)	31(4)	-7(3)	0	0
N2	24(3)	30(3)	35(3)	-5(3)	3(2)	5(2)
C1	32(4)	26(3)	30(3)	4(3)	-4(3)	-3(3)
C2	30(5)	28(5)	27(4)	6(4)	0	0

^a $U_{(\text{eq})}$ is defined as one-third of the trace of the orthogonalized U_{ij} tensor.

Table S7. Selected bond lengths [Å] of **I - III**.

I		II		III	
Bond	Length/Å	Bond	Length/Å	Bond	Length/Å
O1-C1	1.213(6)	O1-C1	1.227(7)	O1-C1	1.205(7)
O2-C2	1.235(8)	O2-C2	1.213(5)	O2-C2	1.232(11)
N1-C1	1.366(5)	N1-C1	1.370(5)	N1-C1	1.384(8)
N2-C1	1.365(6)	N1-C2	1.381(5)	N2-C1	1.359(8)
N2-C2	1.354(5)	N2-C2	1.369(5)	N2-C2	1.372(7)

Table S8. Selected bond angles (°) of **I - III**.

I		II		III	
Angle	(°)	Angle	(°)	Angle	(°)
C2-N2-C1	125.0(5)	C1-N1-C2	125.6(4)	C1-N2-C2	125.8(6)
O1-C1-N1	122.1(4)	O1-C1-N1	122.7(3)	O1-C1-N1	121.2(6)
O1-C1-N2	123.6(5)	O2-C2-N1	122.5(4)	O1-C1-N2	124.3(7)
O2-C2-N2	122.2(3)	O2-C2-N2	124.0(4)	O2-C2-N2	122.8(4)
N2-C1-N1	114.3(5)	N2-C2-N1	113.5(4)	N2-C1-N1	114.6(6)

Table S9. The infrared vibrations and assignments of **I - IV** in detail (Vibrational frequencies/cm⁻¹).

I	II	III	IV	Assignment
415		414		$\delta(\text{N-C-O})$
528	532	524	540	$\delta(\text{C=O})$
646, 692	673	641, 692	690	$\delta(\text{CNC}), \delta(\text{NCO})$
730 - 790	718, 758	730 - 770	769	$\pi(\text{C-O})$
1045	1045	1050	1063	$\nu(\text{C-O})$
1396	1384	1392	1388	$\nu(\text{C-N})$
1462	1446, 1575	1440 - 1580	1475	$\nu(\text{C}_3\text{N}_3)$
1700 - 1790	1710 - 1780	1700 - 1780	1700 - 1790	$\nu(\text{C=O})$
2783, 2851	2762, 2857	2778, 2843	2766, 2867	Hydrogen Bonds
3020 - 3260	3040 - 3140	3030 - 3280	2944, 3103	$\nu(\text{NH})$

2. Supplementary Figures.

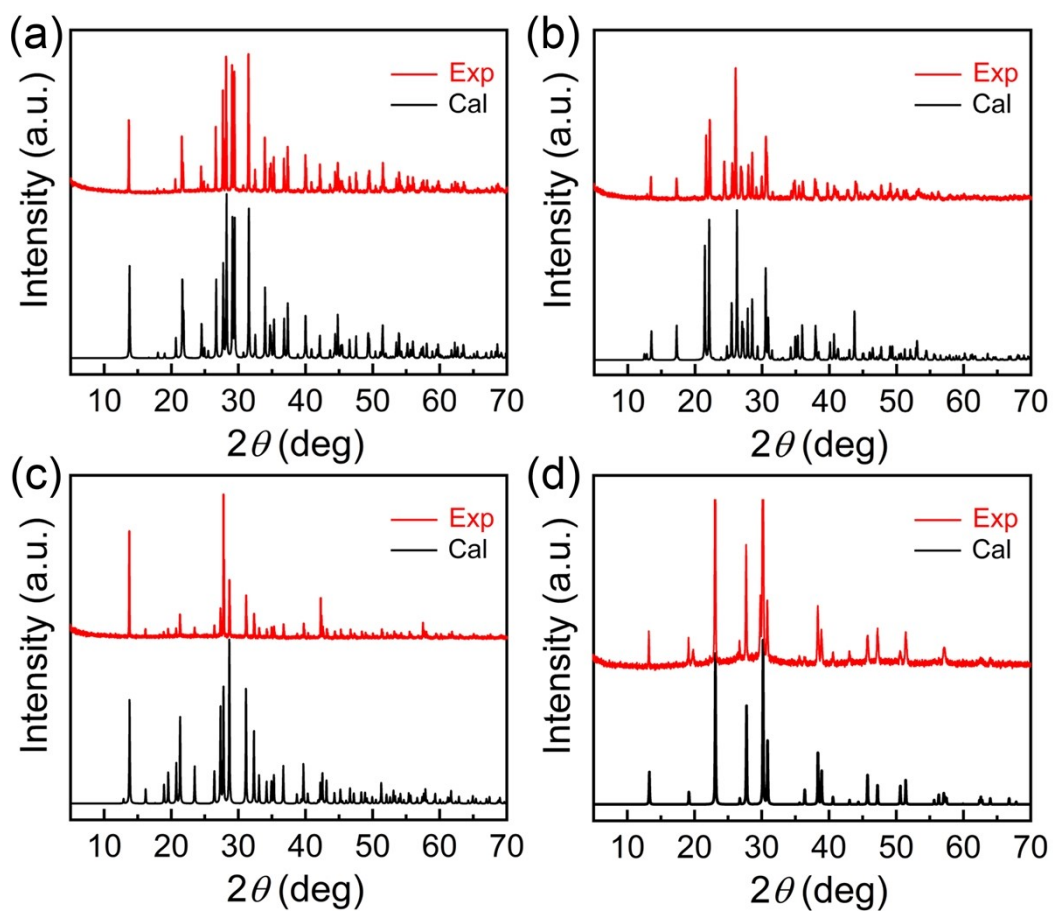


Figure S1. The calculated and experimental PXRD patterns for (a) I, (b) II, (c) III and (d) IV.

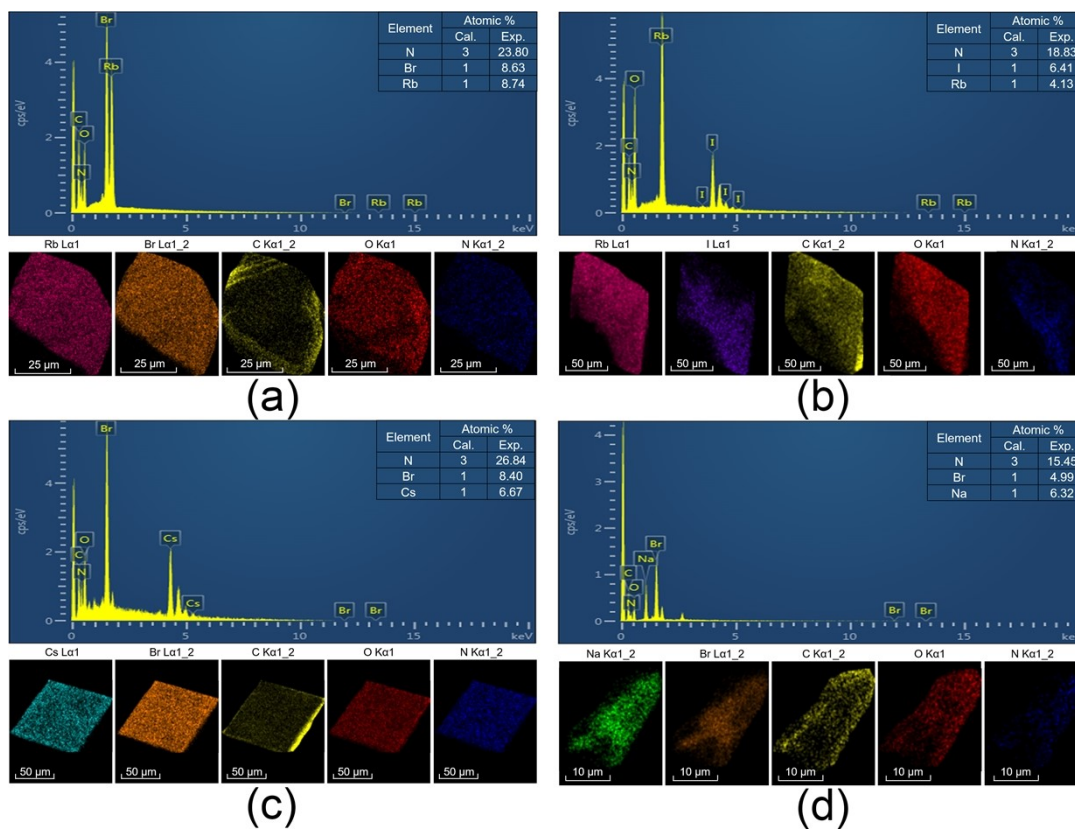


Figure S2. EDS analysis of (a) I, (b) II, (c) III and (d) IV.

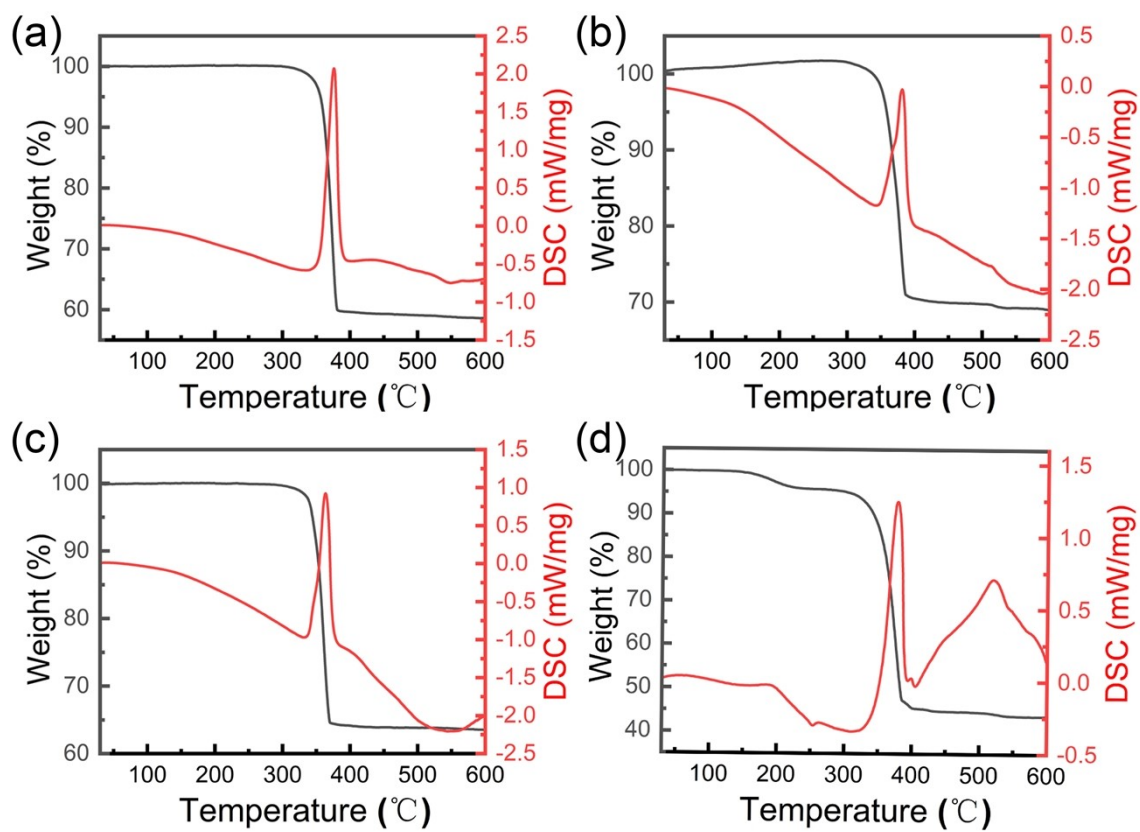


Figure S3. The TG and DSC curves of (a) I, (b) II, (c) III and (d) IV.

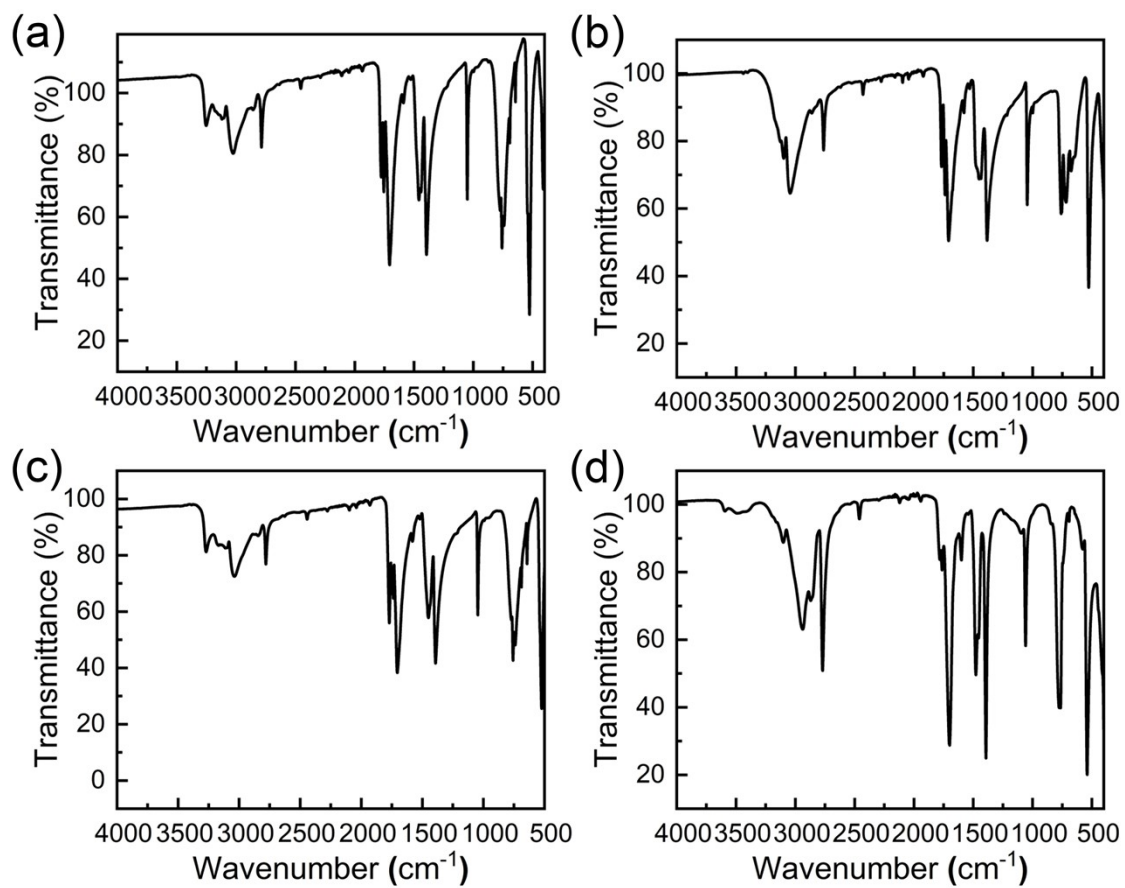


Figure S4. The IR spectra of (a) I, (b) II, (c) III and (d) IV.

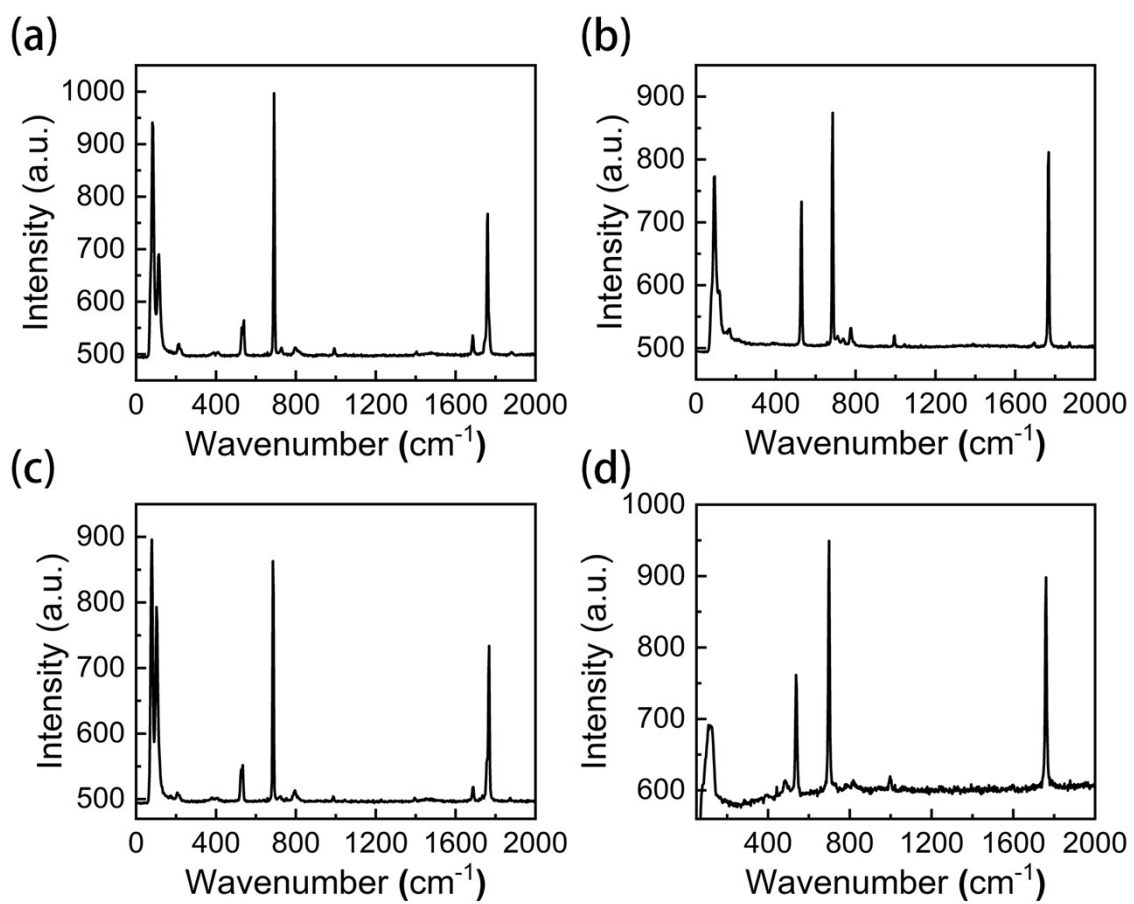


Figure S5. The Raman spectra of (a) **I**, (b) **II**, (c) **III** and (d) **IV**.

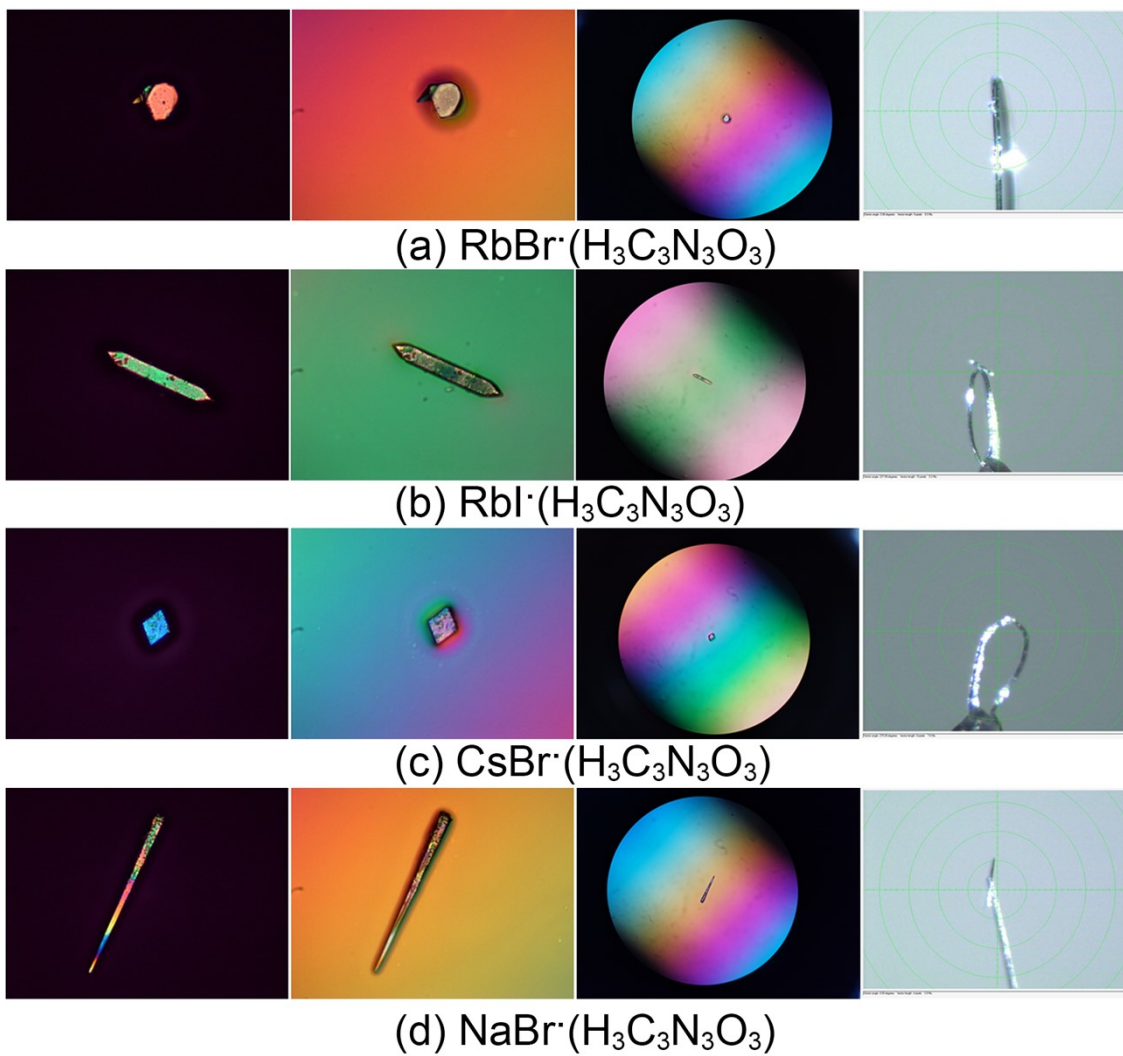


Figure S6. Photographs of crystal (a) I, (b) II, (c) III and (d) IV for the measurement of birefringence.

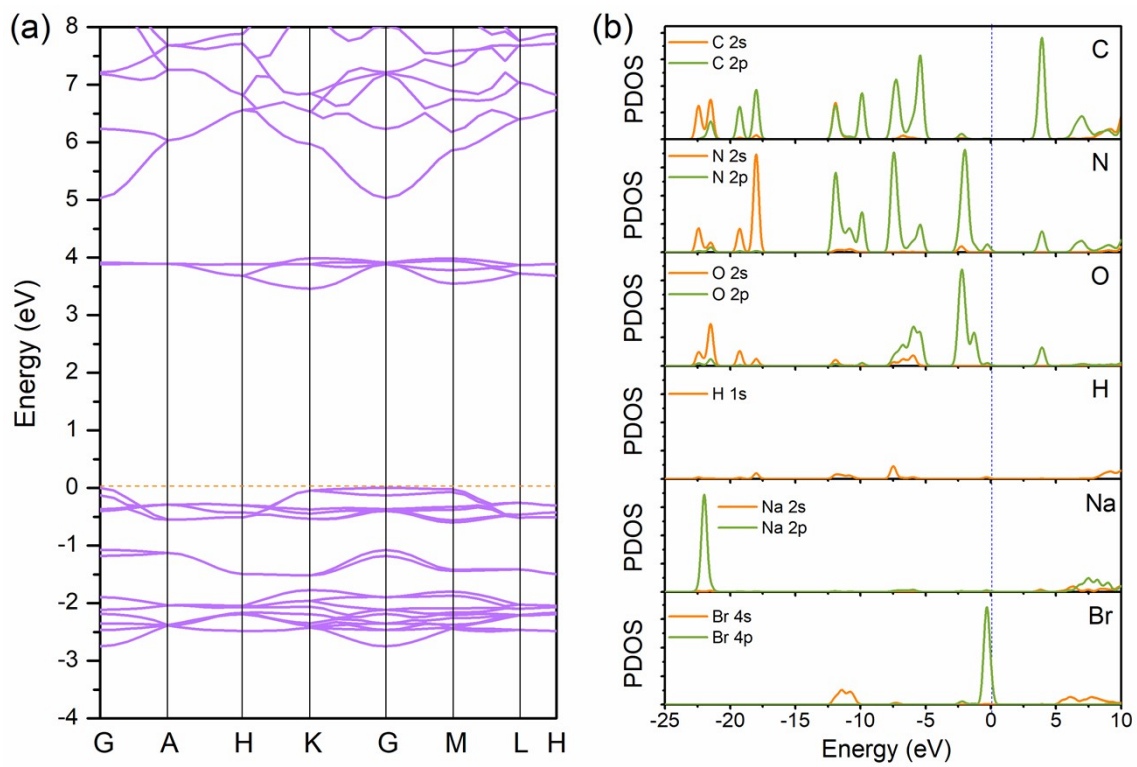
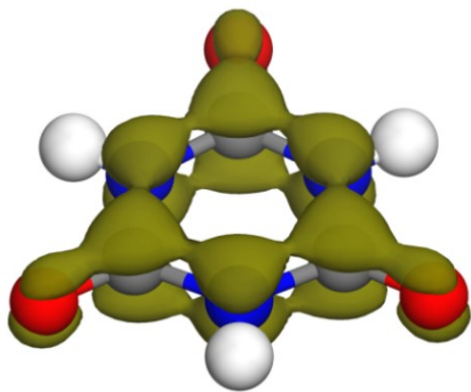
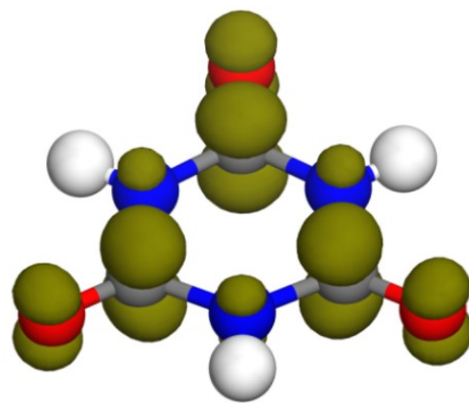


Figure S7. Calculated band structures (a) and the partial density of states of constituent atoms in **IV** (b).



π -bond state



anti- π bond state

Figure S8. The conjugated π -bond state around -5 eV and anti- π bond state around 4 eV on $\text{H}_3\text{C}_3\text{N}_3\text{O}_3$ neutral molecule.

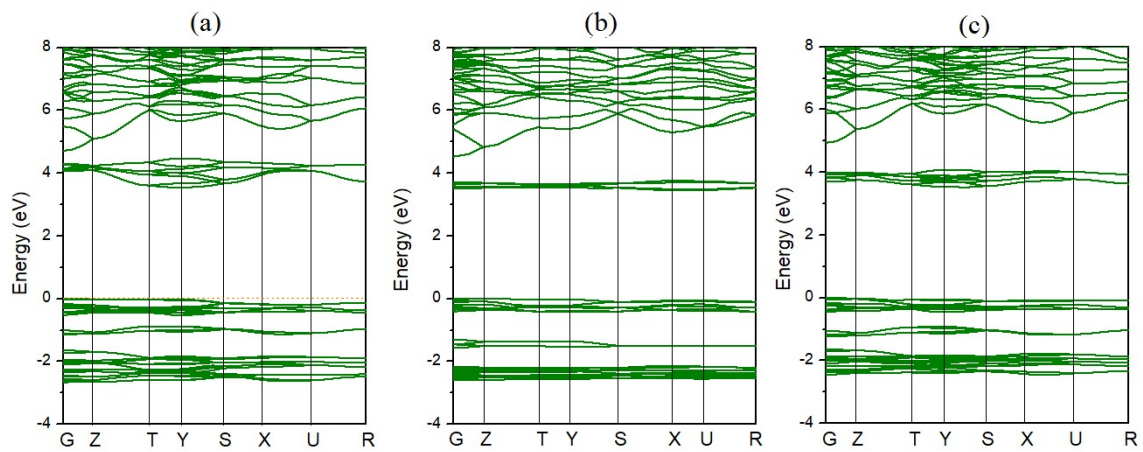


Figure S9. Calculated band structures of (a) **I**, (b) **II** and (c) **III**.

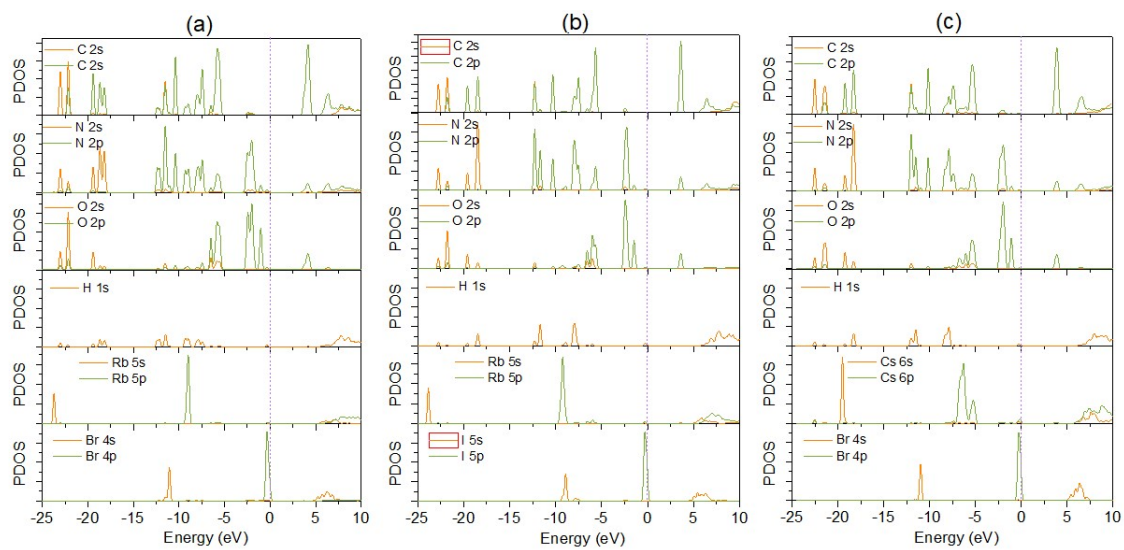


Figure S10. The partial density of states of constituent atoms in (a) **I**, (b) **II** and (c) **III**.

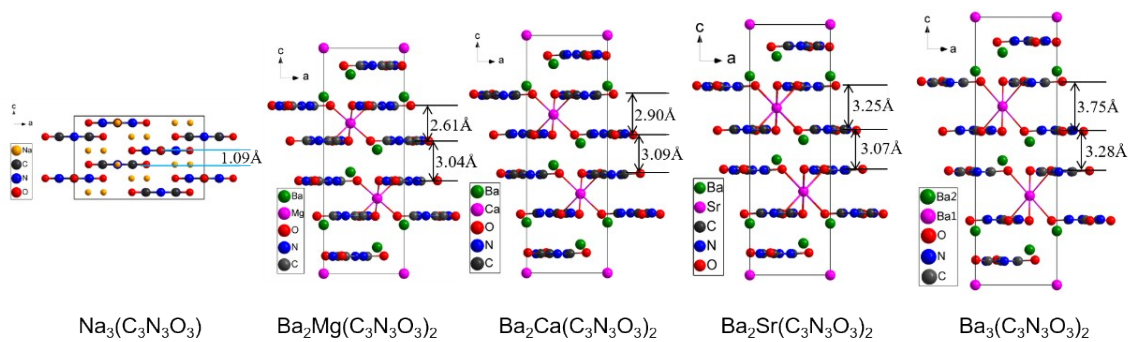


Figure S11. The comparison between $\text{Na}_3(\text{C}_3\text{N}_3\text{O}_3)$ and $\text{Ba}_2\text{M}(\text{C}_3\text{N}_3\text{O}_3)_2$ series ($\text{M} = \text{Mg}, \text{Ca}, \text{Sr}, \text{Ba}$).

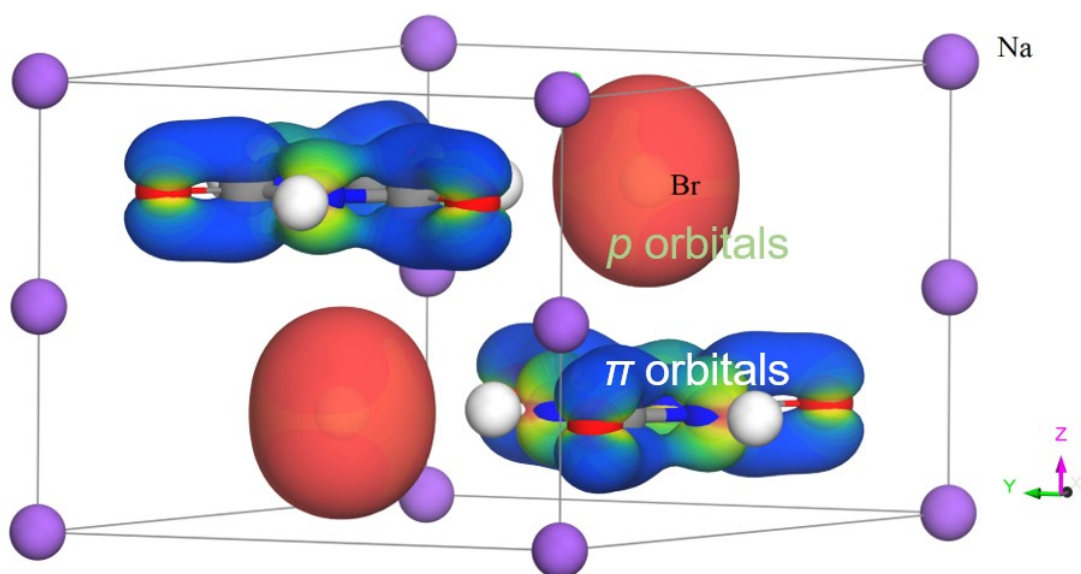


Figure S12. The p - π -interaction between Br $4p$ orbitals and π -bond on cyanuric molecules.

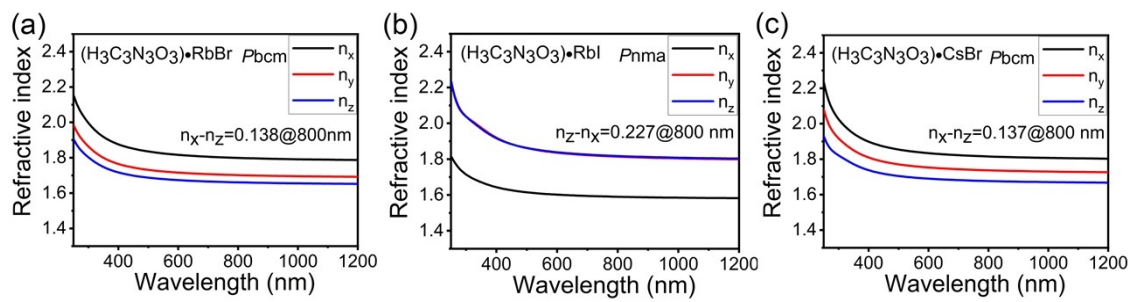


Figure S13. The simulated refractive indexes of (a) I, (b) II and (c) III.